Optimization, performance, and application of a pyrolysis-GC/MS method for the identification of microplastics

Ludovic Hermabessiere, Charlotte Himber, Béatrice Boricaud, Maria Kazour, Rachid Amara, Anne-Laure Cassone, Michel Laurentie, Ika Paul-Pont, Philippe Soudant, Alexandre Dehaut, et al.

Optimization, performance and application of a Pyrolysis-GC/MS method for the identification of microplastics

Article *in* Analytical and Bioanalytical Chemistry · July 2018

DOI: 10.1007/s00216-018-1279-0

CITATIONS
0

READS
159

11 authors, including:

Ludovic Hermabessiere
Agence Nationale de Sécurité Sanitaire de l'Alimentation, de l'Environnement et d…
14 PUBLICATIONS **121** CITATIONS
SEE PROFILE

Charlotte Himber
Agence Nationale de Sécurité Sanitaire de l'Alimentation, de l'Environnement et d…
13 PUBLICATIONS **76** CITATIONS
SEE PROFILE

Rachid Amara
Université du Littoral Côte d'Opale (ULCO)
141 PUBLICATIONS **2,154** CITATIONS
SEE PROFILE

Ika Paul-Pont
Université de Bretagne Occidentale
54 PUBLICATIONS **830** CITATIONS
SEE PROFILE

Optimization, performance and application of a Pyrolysis-GC/MS method for the identification of microplastics

Ludovic HERMABESSIERE[a], Charlotte HIMBER[a], Béatrice BORICAUD[a], Maria KAZOUR[b,c], Rachid AMARA[b], Anne-Laure CASSONE[d], Michel LAURENTIE[e], Ika PAUL-PONT[d], Philippe SOUDANT[d], Alexandre DEHAUT[a,1] & Guillaume DUFLOS[a,1]*

[a] ANSES, Laboratoire de Sécurité des Aliments, Boulevard du Bassin Napoléon, 62200 Boulogne, France

[b] Univ. Littoral Côte d'Opale, CNRS, Univ. Lille, UMR 8187, LOG, Laboratoire d'Océanologie et de Géosciences, 32 Avenue Foch, Wimereux, France

[c] CNRS, National Centre for Marine Sciences, PO Box 534, Batroun, Lebanon.

[d] Laboratoire des Sciences de l'Environnement Marin (LEMAR), UMR6539/UBO/CNRS/IRD/IFREMER, Institut Universitaire Européen de la Mer, Technopôle Brest-Iroise, rue Dumont d'Urville, 29280 Plouzané, France

[e] ANSES, Plateforme PAS, Laboratoire de Fougères, 10 B rue Claude Bourgelat, Javené, 35300 Fougères, France

[1] These authors contributed equally to this work.

* Corresponding author:
guillaume.duflos@anses.fr
+33 3 21 99 25 00

Published in Analytical and Bioanalytical Chemistry and available online at

https://doi.org/10.1007/s00216-018-1279-0

Abstract

Plastics are found to be major debris composing the marine litter, microplastics (MP, <5 mm) being found in all marine compartments. Microplastics number tends to increase with decreasing size leading to a potential misidentification when only visual identification is performed. These last years, pyrolysis coupled with gas chromatography/mass spectrometry (Py-GC/MS) has been used to get information on the composition of polymers with some applications on microplastics identification. The purpose of this work was to optimize and then validate a Py-GC/MS method, determine limit of detection (LOD) for eight common polymers, and apply this method on environmental MP. Optimization on multiple GC parameters was carried out using polyethylene (PE) and polystyrene (PS) microspheres. The optimized Py-GC/MS method require a pyrolysis temperature of 700 °C, a split ratio of 5 and 300 °C as injector temperature. Performance assessment was accomplished by performing repeatability and intermediate precision tests and calculating Limit of Detection (LOD) for common polymers. LOD were all below 1 µg. For performance assessment, identification remains accurate despite a decrease in signal over time. A comparison between identifications performed with Raman micro spectroscopy and with Py-GC/MS was assessed. Finally, the optimized method was applied to environmental samples, including plastics isolated from sea-water surface, beach sediments, and organisms collected in the marine environment. The present method is complementary to µ-Raman spectroscopy as Py-GC/MS identified pigment containing particles as plastic. Moreover, some fibers and all particles from sediment and sea-surface were identified as plastic.

Keywords

Microplastics, Pyrolysis, Gas-chromatography, method, environmental samples

1. Introduction

Plastic is a commonly used material as it is inexpensive, strong, lightweight, and easy to manufacture [1]. Plastic production increased from the 1950's and reached 335 million metric tons in 2016 [2]. Due to waste management issues and incivilities, it has been estimated that 5 to 12 million plastic particles end up in Oceans in 2010 [3]. Low estimates predicted that floating marine plastic weight between 70,000 and 270,000 tons [4-6], thus, potentially representing more than 51 trillion plastic pieces in Oceans [6].

Microplastics (MP) are plastic particles smaller than 5 mm in their longest size [7]. To date, multiple studies are carried out to quantify MP in sediments, in water column, and in organisms from both freshwater and marine environments [8, 9]. For large MP (1-5 mm) [10] and macroplastic (>5 mm), visual identification relying on physical characteristics is possible but the proportion of misidentification grows with decreasing particles size [11]. However, some studies still do not perform any characterization of MP based on their chemical composition [12]. Additionally, as plastic materials include a large variety of polymers, more than 5,000 grades [13], chemical identification is now mandatory to ensure the accuracy of collected pollution data [14]. Raman and Fourier-Transform Infrared (FTIR) spectroscopies are the most common techniques employed to identify polymer types of MP [15]. Furthermore, the use of imaging techniques coupled to spectroscopic approaches allows automatization of MP identification [16-18]. In addition to spectroscopic methods, another type of chemical identification is thermal analysis [12]. Pyrolysis-Gas Chromatography coupled with Mass Spectrometry (Py-GC/MS) is one of the thermal analysis techniques used to identify MP polymers. Py-GC/MS has been used to identify MP from different matrix based on their thermal degradation products [19-25]. Furthermore, Py-GC/MS allows the analysis of a whole MP particle in contrast with Raman or FTIR (in reflection mode) which

only analyze the surface of the MP particle being sensitive to interference caused by additives such as pigments [26-28], for example.

To date, studies using Py-GC/MS to identify the polymeric composition of MP document neither the method development nor the assessment of its performance. Some authors stated that Py-GC/MS is only feasible with MP >500 µm [29, 30] even if so far, 100 µm is the smallest size of an isolated MP that has been identified [19]. Recently, particles smaller than 1 µm, referred as nanoplastics by the authors, have been identified as plastics based on Py-GC/MS and statistical approaches in bulk samples from the North Atlantic Subtropical Gyre [31].

The purpose of this work was fourfolds: (i) optimize a Py-GC/MS method to accurately identify polymer of MP, (ii) assess the performance of the Py-GC/MS approach, (iii) compare identifications with samples already identified by µ-Raman and (iv) apply this technique to environmental samples.

2. Material and methods

2.1. Reference material

Microspheres with calibrated size ranges were purchased for the Py-GC/MS optimization method. Polyethylene (PE) (180-212 µm; reference: CPMS-0.96 180-212um) and Poly(Methyl Methacrylate) (PMMA) (180-212 µm; reference: PMMAMS-1.2 180-212um) microspheres were acquired from Cospheric LLC (Santa Barbara, USA) and Polystyrene (PS) (106-125 µm; reference: 198241) from Polysciences Europe GmbH (Hirschberg an der Bergstrasse, Germany). For the calculation of the LOD, other polymers were bought from Goodfellow (Lille, France) including filaments of polycaprolactam (PA-6), polyethylene

93 terephthalate (PET) and polypropylene (PP) and fragments of polycarbonate (PC) and
94 unplasticized polyvinyl chloride (uPVC).

95 For all polymers, characteristic compounds are presented in Table 1 (see Electronic
96 Supplementary Material Figure S1 to S8) and were choose according to their
97 representativeness for polymer identification, their relative intensity, and in comparison with
98 the literature [22, 32, 33].

99

100 **Table 1 Polymer related pyrogram information**

Polymer	Characteristic compound[a]	LRI[b]	Indicator ion (m/z)
PE	1-Nonene (C9)	893	83; 97
	1-Decene (C10)	993	83; 97
	1-Undecene (C11)	1093	83; 97
	1-Dodecene (C12)	1192	83; 97
	1-Tridecene (C13)	1292	83; 97
	1-Tetradecene (C14)	1392	83; 97
	1-Pentadecene (C15)	1492	83; 97
	1-Hexadecene (C16)	1578	83; 97
PS	**Styrene**	898	78; 104
	3-butene-1,3-diyldibenzene (styrene dimer)	1733	91; 208
PMMA	**Methyl methacrylate**	743	41; 69; 100
PP	**2;4-dimethyl-1-heptene**	846	70
PA-6	**ε-caprolactam**	1274	113
PC	Phenol	980	66; 94
	p-Cresol	1075	77; 107
	p-Ethylphenol	1168	107; 122
	p-Vinylphenol	1217	91; 120
	p-Isopropenylphenol	1304	119; 134
	Bisphenol A	2088	213; 228
PET	Benzene	770	52; 78
	Acetophenone	1076	51; 77; 105
	Vinyl benzoate	1145	52; 77; 105
	Benzoic acid	1178	77; 105; 122
	Divinyl terephthalate	1574	104; 175
uPVC	Benzene	770	52; 78
	Toluene	782	91
	Styrene	898	78; 104
	Indene	1059	116
	Naphthalene	1206	128
	2-methylnaphthalene	1320	115; 142
	1-methylnaphthalene	1340	115; 142

[a] Marker compounds in bold were used to calculate Limit of Detection;
[b] Retention Index were calculated according to van Den Dool and Kratz [34]; m/z: mass to charge ratio

2.2. Sample preparation

Each particle was selected based on its size (*ca*. 200 µm) under a SZ61 stereomicroscope (Olympus, Rungis, France) and then introduced into an analysis cup (Frontier-Lab, Fukushima, Japan) for Py-GC/MS analysis. All analysis cup used in this work were brand new cups visually controlled prior to analysis to detect any possible contamination.

2.3. Size and weight estimation

In order to estimate the size of the particle, a photograph was taken with a scale bar using a DP21 camera (Olympus, Rungis, France) mounted on the stereomicroscope. The size in pixel of the particle was recorded using GIMP 2 software (2.8.16). Then, the maximum size in µm of the particle was calculated using the scale bar. For each particle, the volume (cm^3) was estimated using different formula (1), (2) or (3), where D corresponds to the diameter, L to the length and S to the side size (see Electronic Supplementary Material Weight estimation). The volume was then multiplied by the density (g/cm^3) of the polymer to obtain the estimated weight.

$$(1)\ Microsphere\ volume = \frac{4}{3} \times \pi \times (\frac{D}{2})^3$$

$$(2)\ Filament\ volume = (\frac{D}{2})^2 \times \pi \times L$$

$$(3)\ Fragment\ volume = S^2 \times L$$

2.4. Method optimization

2.4.1. Initial Py-GC/MS method

The hereafter called “initial method” was described by Dehaut et al. [35]. Briefly, the analysis cup containing the plastic was placed on the AS-1020E autosampler of an EGA/PY-3030D device (Frontier Lab, Fukushima, Japan). Samples were pyrolysed at 600 °C for 1 min.

Pyrolysis products were injected with a split of 20, on a GC-2010 device (Shimadzu, Noisiel, France) equipped by a RXi-5ms® column (60 m, 0.25 mm, 25 µm thickness) (Restek, Lisses, France). Temperatures of the pyrolyzer interface and the injection port were both set at 300 °C. Helium was used as a carrier gas with a linear velocity of 40 cm/s. The initial oven program, called here after **program 0**, was set as follows: 40 °C for 2 min, then increase to 320 °C at 20 °C/min, maintained for 14 min. Mass spectra were obtained by a Shimadzu QP2010-Plus mass spectrometer. Interface temperature was set at 300 °C, ion source temperature was set at 200 °C, ionization voltage was set at 70 eV, and a mass range from 33 to 500 m/z was scanned at 2000 Hz.

As a primary attempt, polymer identification was realized using total ion pyrogram (TIC) which was firstly identified using F-Search software 4.3, querying pyrograms against Frontier Lab's database, and our own database containing pre-established pyrograms with plastic samples. Identification was established based on the similarity percentage (minimum value of 80%) between average mass spectra on the whole chromatogram. Our home-made database was created using our '"initial method" and the optimized Py-GC/MS method on plastic references from Goodfellow (Lille, France). Plastic references used for our home-made database included: PE, PS, PP, PET, PA-6, PC, PMMA and uPVC.

When identification was not possible after primary attempt, a classical GC/MS treatment was performed. Peaks of pyrograms were integrated and compared with available literature [32] or characteristic compounds (Table 1), single peak identification being carried out using NIST08 database and LRI.

2.4.2. Pyrolysis temperature

Optimization of the pyrolysis temperature was carried out using the initial pyrolysis method. The impact of pyrolysis temperature was determined using five replicate of PE microspheres. Three additional pyrolysis temperatures were tested: 500, 700 and 800 °C for 1 min.

2.4.3. GC oven temperature program

In addition to **Program 0**, two others temperature programs were tested. **Program 1** was set as follow: 40 °C for 2 min, then increase to 200 °C at 15 °C/min followed by a second increase to 300 °C at 10 °C/min maintained for 2 min. **Program 2** was set as follow: 40 °C for 2 min, then increase to 261 °C at 13 °C/min followed by a second increase to 300 °C at 6 °C/min maintained for 2 min. Except pyrolysis temperature was set at 700 °C the optimal temperature for 1 min (*cf.* 3.1.1), oven program was the unique parameter modified in this part, other parameters were conserved as those of the initial method. The impact of GC oven temperature program on resolution was determined using PE microspheres. Here the resolution was only used to assess the separation between PE alkene and alkadiene. The resolution of alkenes (from C_9 to C_{16}) was used to evaluate each program performance. Resolution was calculated by the Shimadzu GC-MS postrun analysis software using (4), where T_r corresponds to the retention time of the considered peak (Alkene), T_{rp} to the retention time of the previous peak (Alkadiene), W to the width of the considered peak and W_p to the width of the previous peak:

$$(4)\ Resolution = 2 \times \frac{T_r - T_{rp}}{W + W_p}$$

Five replicates were performed per programs.

2.4.4. Injector temperature and split ratio

Optimization on the split ratio and injector temperature was performed using PE and PS microspheres. Here, PS was used in addition to PE as this polymer exhibits only a few degradation products after pyrolysis (Table 1). Three split ratios (50, 20 and 5) and three injector temperatures (280, 300 and 320 °C) were applied, resulting in nine distinct combinations. For all combinations, pyrolysis temperature and GC oven program were set following the previous optimization steps, others parameters were conserved as those described for the initial method (*cf.* 2.4.1). For each combination, five microspheres of PE and PS were analyzed.

2.5. Method performance evaluation

Split ratios were adjusted to ensure that no saturation of the mass spectrum occured. To do so, split ratio was set at 5 for PE microspheres, particles identified by µ-Raman spectroscopy, and unknown particles injection, whereas for PMMA and PS microspheres injection, a split of 50 was chosen.

2.5.1. Repeatability and intermediate precision

For repeatability and intermediate precision, respectively ten and five microspheres of the three polymers were pyrolysed and the Relative Standard Deviation (RSD) (5) was calculated for each characteristic peak according to ISO 5725-3 [36] where s is the standard deviation and m is the mean:

$$(5)\ RSD\ (\%) = \frac{s}{m} \times 100$$

Intermediate precision was assessed over time with pyrolysis occurring at 3, 4 and 6 weeks after repeatability experiences. The method is considered valid if RSD is below 20 % for repeatability and intermediate precision. Moreover, polymer identification of the particles was performed as previously described (*cf.* 2.4.1) to obtain qualitative data.

2.5.2. Limit of detection

Limit of detection was calculated according to Caporal-Gautier et al. [37]. First, ten analysis cups without plastic, hereafter referred as "blank", were pyrolysed. For each blank and at the retention time of each characteristic peak of the eight used polymers (Table 1), the maximum height was determined over a time interval equal to 20 times the full width at half maximum (FWHM), this area is called H_{20FWHM}. Interval surrounds the retention time of each peak with the retention time being the central point of the time range. Five particles were pyrolysed for each polymer. A response factor (R) (6) was calculated: "Weight" corresponds to the mean the average calculated weight and "Height" corresponds to the mean height of the characteristic peak for the five particles:

$$(6)\ Response\ factor\ (R) = \frac{Weight}{Height}$$

Finally, for each polymer LOD were calculated as follow:

$$(7)\ Limit\ of\ Detection\ (LOD) = 3\ \times R\ \times\ H_{20\mathrm{FWHM}}$$

2.6. Method comparison

2.6.1. Sampling

Unknown plastic particles were first analysed by µ-Raman and then by Py-GC/MS before identification to be compared. Comparison of the identification of unknown plastic particles obtained after µ-Raman spectroscopy and Py-GC/MS was performed. To assess methods comparison, fifty plastic particles hand sampled on a local beach (Equihen Plage, France – 50°39'51.08″N, 1°34'17.94″E) were used.

2.6.2. Identification by µ-Raman and Py-GC/MS

For µ-Raman analysis, each particle was analyzed with an XploRA PLUS V1.2 (HORIBA Scientific, France SAS) equipped with two lasers of 785 and 532 nm wavelength. First, plastic

205 particles were analyzed with laser wavelength set at 785 nm over a range of 50 to 3,940 cm^{-1}
206 with a x10 (NA=0.25; WD=10.6 mm) or x100 (NA=0.9; WD=0.21 mm) objective (Olympus,
207 France). If identification with the 785 nm laser was not successful, particles were secondly
208 analyzed with a laser wavelength set at 532 nm over a range of 50 to 4,000 cm^{-1} with a x10 or
209 x100 objective. The experimental conditions (integration time, accumulation, laser power)
210 were adapted to limit fluorescence and increase the spectral quality of the analyzed particles.
211 Polymer identification was carried out using spectroscopy software (KnowItAll, Bio-Rad) and
212 our own database containing pre-established polymers spectra. Identification was considered
213 correct if Hit Quality Index (HQI) was above 80 (ranging from 0 to 100). If identification of a
214 particle was not successful after µ-Raman spectroscopy, the particle was then included in the
215 section 2.7.

216 For Py-GC/MS, a piece of each particle was cut to the smallest possible size and prepared as
217 indicated in section 2.2. Pyrolysis-GC/MS was realized as described above (*cf.* 2.5).

218 **2.7. Application: identification of unknown particles**

219 **2.7.1. Sampling**

220 Application of the Py-GC/MS was performed using particles collected on a beach, extracted
221 from bivalves and collected on sea surface waters.

222 Ten particles, collected by hand on a local beach, including 4 particles identified as pigment
223 and 6 particles unidentified (*cf.* 3.3) were analyzed using Py-GC/MS.

224 Mussels (*Mytilus edulis*) and cockles (*Cerastoderma edule*) were respectively sampled during
225 morning low tides at Le Portel, France (50°42'30.02"N, 1°33'34.43"E) on 10/29/2015 and at
226 Baie d'Authie, France (50°22'17.22"N, 1°35'4.8"E) on 11/15/2015. Bivalves were then
227 dissected, digested, and filtered using the method of Dehaut et al, [35]. Particles resembling
228 plastic found in bivalves were extracted under a stereomicroscope using tweezers and

submitted to µ-Raman identification using an LabRam HR800 (HORIBA Scientific, Villeneuve d'Ascq, France) following a methodology adapted from Frère et al, [16]. Here, 16 particles from bivalves, previously identified as pigments containing particles, and 10 unknown particles in form of fibers were analyzed. Finally, 24 unknown particles collected in sea-surface trawls from the bay of Brest, as described by Frère et al. [38], were used for identification by Py-GC/MS.

2.7.2. Identification by Pyrolysis-GC/MS

In total, sixty particles with no previous polymer identification were analyzed. For Py-GC/MS, a piece of each particle was cut to the smallest size possible and prepared as indicated in section 2.2. Pyrolysis-GC/MS was realized as described above (*cf.* 2.5). Results will be present and discuss according to the following categories: pigments containing particles, fibers and others particles.

2.8. Statistical analyses

All statistical analyses with an exception for RSD calculation were performed using R (3.4.0) [39]. For method optimization, including verification of estimated size of microspheres used, normality and homoscedasticity of the distribution hypothesis were carefully verified before performing ANOVA. Assuming one of the hypothesis was not verified, a Kruskal-Wallis test was carried out. Kruskal-Wallis tests were followed by a conservative post-hoc test using the Fisher's least significant difference (LSD) criterion and Bonferroni correction. Post-hoc tests were performed using the agricolae package (1.2-7) [40]. All results are expressed as a mean ± 2 standard error (S.E), representing the 95% confidence interval (95% CI). Differences were considered significant when $p\text{-value}<0.05$. On bar charts, two different letters illustrates significantly different value with a 95% CI.

3. Results and discussion

All procedural blank, *i.e* analysis cup without sample, presented no sign of contamination by pyrolytic products of synthetic polymers.

3.1. Method optimization

3.1.1. Pyrolysis temperature

PE microspheres size (204 to 214 μm) used for optimizing the pyrolysis temperature were not significantly different for each tested temperatures (One-way ANOVA, $p>0.05$). Pyrolysis temperature (500, 600, 700 and 800 °C) had a significant impact on the peaks areas of PE (Fig. 1). On the one hand, for the eight characteristic compounds of PE, peaks areas rises when the pyrolysis temperature increase from 500 to 700 °C but on the other hand at 800 °C, peaks areas slightly decreased (Fig. 1). Moreover, significant difference of areas were recorded for characteristic compounds of PE (Kruskal-Wallis, $p<0.05$). Areas were significantly higher at 700 °C in comparison with areas at 500 °C (Kruskal-Wallis followed by post-hoc, $p<0.05$ – Fig. 1). Significant differences between areas at 600 and 700 °C were observed for 1-Nonene, 1-Decene, 1-Undecene, 1-Dodecene, and 1-Tridecene (Kruskal-Wallis followed by post-hoc, $p<0.05$ – Fig. 1). However, no significant difference was observed between 500 and 600 °C, between 700 and 800 °C, and between 600 and 800 °C for all 8 characteristics compounds (Kruskal-Wallis followed by post-hoc, $p<0.05$ – Fig. 1). At 800 °C, pyrograms of PE microspheres were not all typical with the presence of unknown compounds at the beginning of the pyrogram which lead to identification with a percentage below 80 % (see Electronic Supplementary Material Figure S9). As 700 °C demonstrated higher areas for characteristic compounds of PE with typical and clearly identified pyrograms; optimal pyrolysis was then set at 700 °C.

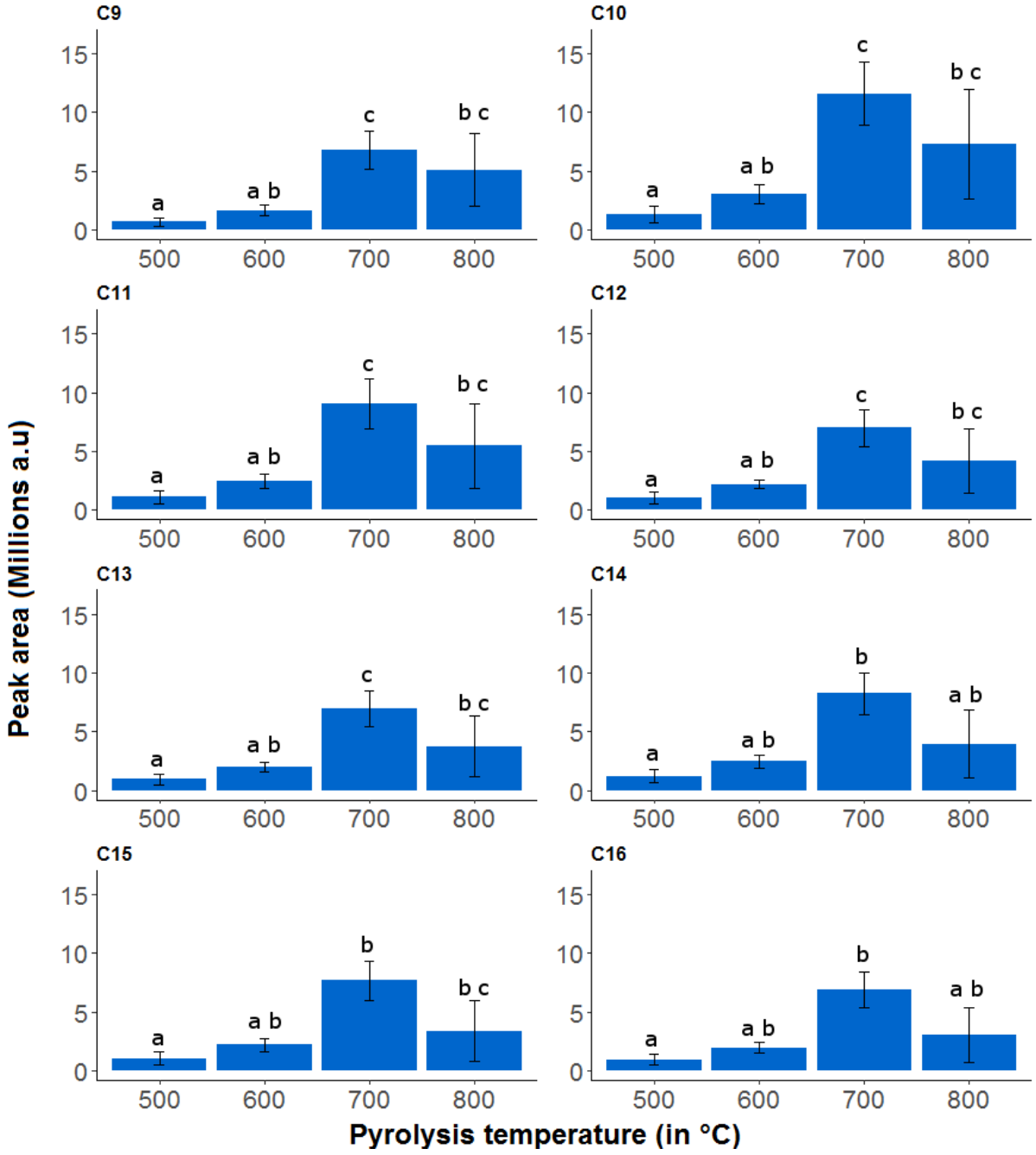

Fig. 1 Peaks areas (Arbitrary Unit) depending on the Pyrolysis temperature (in °C) for eight characteristic compounds of PE. Values as expressed as mean ± 95 % confidence interval. Letters correspond to the differences after post-hoc test using the Fisher's least significant difference with Bonferroni correction. C9: 1-Nonene; C10: 1-Decene; C11: 1-Undecene; C12: 1-Dodecene; C13: 1-Tridecene; C14: 1-Tetradecene; C15: 1-Pentadecene; C16: 1-Hexadecene

Regarding the literature, studies generally used a pyrolysis temperature of 700 °C [19-21, 23, 31, 33] while others used lower temperature such as 550 °C [24], 590 °C [22], 600 °C [32, 35] or 650 °C [25]. As presented in this work, pyrolysis temperature had a clear impact on the signal of the pyrolytic products of PE and could potentially impact identification for small

particles. Additionally, pyrolysis at a temperature greater than or equal to 800 °C had a negative effect on PE pyrolytic products. Indeed, the signal was decreased and the polymer identification was not possible with our software due to the presence of a large interfering peak at the beginning of the pyrogram (see Electronic Supplementary Material Figure S9). Moreover, as indicated by Kusch [33], pyrolysis temperature could also impact the generated pyrolysis products. Here for PC, PET, and uPVC some pyrolysis products were different from those recorded with the initial Py-GC/MS method [35] and from a reference book [32]. Such differences could prevent identification of these polymers as many libraries were obtained after pyrolysis at 600 °C. However, the use of our own database create with pyrolysis temperature set at 700 °C allow accurate polymer identification.

3.1.2. GC oven temperature program

PE microspheres size (197 to 226 µm) used for the optimization of the GC oven temperature program were not significantly different for each tested conditions (One-way ANOVA, $p>0.05$). For all characteristic compounds of PE and for the three GC oven temperature programs, resolution was above 1.5 (see Electronic Supplementary Material Figure S10) which is acceptable [41]. Significant differences in resolution were observed for all peaks of PE (Kruskal-Wallis, $p<0.01$) depending on the used GC oven temperature program. Moreover, program 2 demonstrated higher resolution in comparison with program 0 and 1 (Kruskal-Wallis followed by Fisher's LSD with Bonferroni correction, $p<0.05$ – see Electronic Supplementary Material Figure S10). Here, resolution and peak separation was higher when ramping temperature decrease. Higher peak resolution could be useful for manual identification of peaks, if primary attempt using F-Search software is not conclusive. Program 2 was then applied to perform separation of pyrolysis compounds using the GC system.

3.1.3. Injector temperature and split ratio

PS (110 to 136 µm) and PE (188 to 223 µm) microspheres size used for the optimization on split ratio and injection temperature were not significantly different for each tested conditions (One-way ANOVA, $p>0.05$). For all characteristic compounds of PE, areas significantly decreased with the increase of split ratio (Kruskal-Wallis followed post-hoc, $p<0.05$ – Fig. 2). Moreover, no significant difference in peaks areas were observed at split ratio of 20 and 50 depending on the injector temperature used (Kruskal-Wallis, $p>0.05$). However, it should be noticed that significant differences between injection at 280, 300, and 320 °C were observed using a split ratio of 5 for all characteristic compounds (Kruskal-Wallis followed by post-hoc, $p<0.05$ – Fig. 2). Indeed, with the exception of 1-Nonene, the highest peaks areas were obtained when injector temperature was set at 300 °C with a split ratio of 5 (Fig. 2).

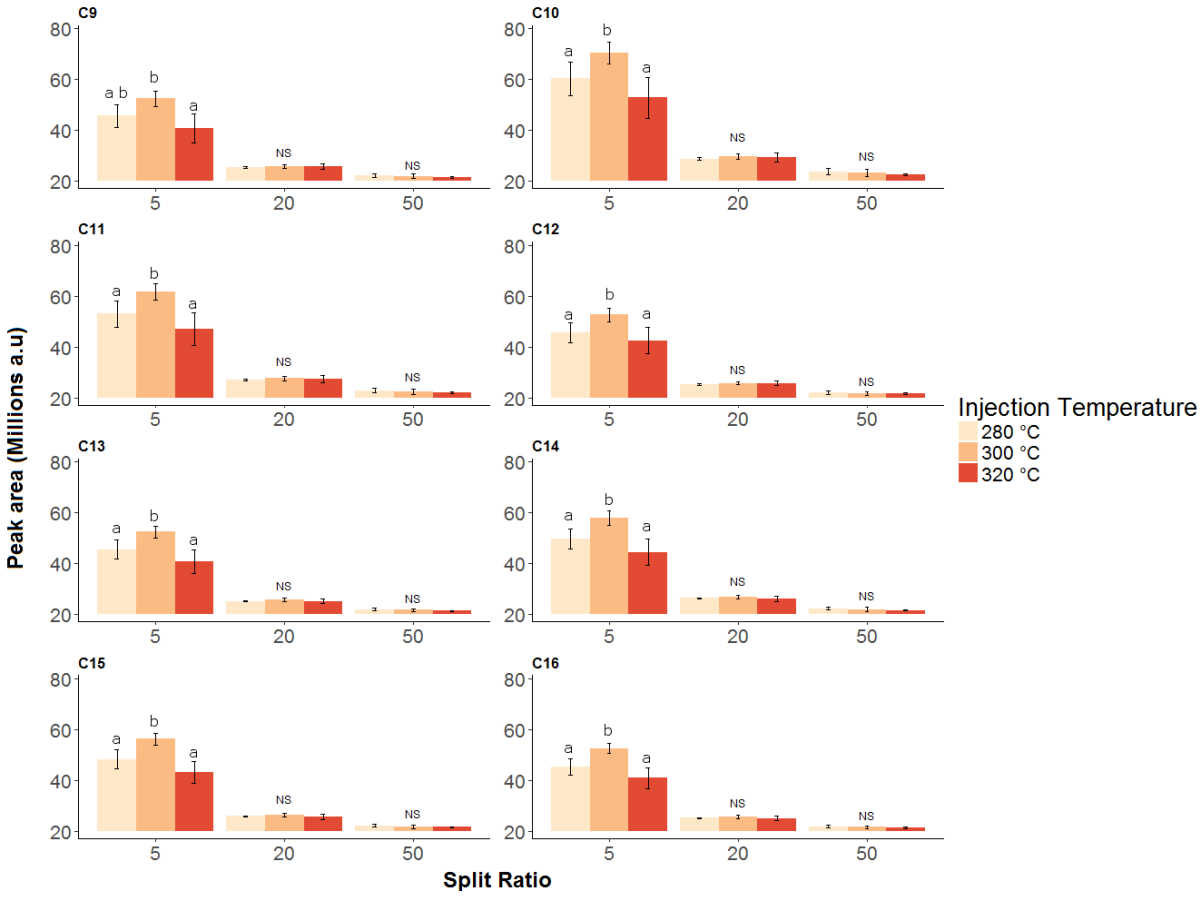

Fig. 2 Peaks areas (Arbitrary Unit) depending on the split ratio and injection temperature for 8 characteristics compounds of PE. Values as expressed as mean ± 95 % confidence interval. Letters

correspond to the differences after post-hoc test using the Fisher's least significant difference with Bonferroni correction and NS stand for non-significant. C9: 1-Nonene; C10: 1-Decene; C11: 1-Undecene; C12: 1-Dodecene; C13: 1-Tridecene; C14: 1-Tetradecene; C15: 1-Pentadecene; C16: 1-Hexadecene

For PS, as for PE, increasing split ratio decreased peaks areas (Kruskal-Wallis, $p<0.01$ – see Electronic Supplementary Material Figure S11). For styrene, at a split ratio of 5, areas were significantly different between 320 °C and the others temperatures (Kruskal-Wallis followed by post-hoc, $p<0.05$ – see Electronic Supplementary Material Figure S11) and at a split ratio of 20, areas were significantly different between 280 and 320 °C (Kruskal-Wallis followed by post-hoc, $p<0.05$ – see Electronic Supplementary Material S11). However, no significant difference were observed for area values at a split ratio of 50 between injector temperatures (Kruskal-Wallis, $p<0.05$). No significant difference were observed for styrene dimer areas between injector temperatures at each split ratio (Kruskal-Wallis, $p>0.05$).

As split ratio is inversely related to the amounts of sample entering the column, such results were expected. Generally, studies using Py-GC/MS to identify MP used low split ratio to increase analyte signal. Indeed, splitless mode was used for injection by severals authors [19-21, 24] while split ratio of 10 [25] or 15 [22] were used by others authors. In several works, split ratio was adapted depending on the weight of the particle to identify [24, 31]. Indeed, Ter Halle et al, [31] used a split ratio of 5 for nanoplastics (25 mg of lyophilizate), 10 for micrometric plastic (particle on filter) and 100 for meso and microplastics and commercial plastics (approximately 10 µg). In addition, in their work Hendrickson et al, [24] used the splitless mode for particles <20 µg and a split ratio of 100 for particles >20 µg. In the others studies few or no information are available on the size or the weight of MP used for Pyrolysis [19, 21, 22, 25]. Here, split ratios tested were between 5 and 50 to be around the split ratio used in our previous work [35] and in order to obtain area for PE characteristic peak above a million of arbitrary unit allowing correct identification using the software. With this optimized Py-GC/MS method, split ratio should also be adapted depending on the weight of

particles. Indeed, for unknown particles smaller than 5 µg a split ratio of 5 should be used and for particles heavier than 5 µg, split ratio should be set at 20. Moreover, injector temperature of 300 °C in combination with split ratio of 5 had a significant effect on peaks areas for all PE's peaks and for styrene from PS (Fig. 2 & see Electronic Supplementary Material Figure S11) which could be important to detect small particles. Here an injection temperature set at 300 °C was chosen for performance assessment purpose.

Globally, method optimization is an important step for the detection and then the identification of MP using Py-GC/MS. Indeed, the higher the signal will be, the higher the probability of identification will be but mass spectrum saturation should be avoided to ensure proper identification. Moreover, MP signal tend to increase with an increasing size of the particle.

3.2. Method performance evaluation

3.2.1. Method repeatability and intermediate precision

PE, PMMA, and PS microspheres used for assessing method repeatability and intermediate precision did not display significant difference in sizes (One-way ANOVA or Kruskal-Wallis, $p>0.05$). Firstly, polymer identifications were, over the 6 weeks period, accurate with similarity percentage all above 90 %. Identification was successful in all cases and the method could be considered repeatable within a week and precise over the 6 weeks. Concerning the repeatability RSD, values were below 20 % for the characteristic compounds of PE and PMMA and above 20 % for characteristics compounds of PS (Table 2). For styrene dimer, highly variable peak areas were recorded for repeatability test. In addition RSD value above 20% for styrene was due to one repetition that presents peak area 1.5 higher in comparison with others replicates. Then, concerning intermediate precision RSD values were above 20 % for all characteristics compounds of PE, PS, and PMMA (Table 2). Consequently, the method

is repeatable for PE and PMMA but not precise over time for all the three tested polymers, regarding quantitative data. Depending on when the analysis was performed, a high variation in peak areas was recorded and thus was responsible for high values of RSD. Indeed, at weeks 1, 3 and 4, areas of characteristics peaks were in the same order of magnitude (for an example see see Electronic Supplementary Material Figure S12). However at week 6, an important diminution of the signal was observed (see Electronic Supplementary Material Figure S12) which can cause the high variability in RSD values for method intermediate precision. Finally, despite a decrease over time in peaks areas for characteristic compounds of PE, PS and PMMA, identifications remained exact. This is essential for future use of the optimized Py-GC/MS method to identify MP.

Table 2 Relative standard deviation (in %) for method repeatability (n=10) and intermediate precision (n=20) for characteristics compounds of Polyethylene, Polystyrene and Poly(Methyl Methacrylate)

Polymer	Characteristic compound	Repeatability RSD (%)	Intermediate Precision RSD (%)
PE	1-Nonene	10,67	31.82
	1-Decene	9,91	31.34
	1-Undecene	10,01	31.79
	1-Dodecene	9,55	31.40
	1-Tridecene	9,06	33.11
	1-Tetradecene	8,81	30.22
	1-Pentadecene	8,98	30.88
	1-Hexadecene	9,62	30.76
PS	Styrene	22,47	32.57
	3-butene-1,3-diyldibenzene (styrene dimer)	48,03	49.69
PMMA	Methyl methacrylate	9,19	24.34

3.2.2. Limit of Detection

The estimated LOD were below 1 µg for all tested polymers using the optimized Py-GC/MS (Table 3). Detection of smaller particles of polymers with a few peaks, such as PS or PMMA could be easier compared to PE which presents numerous pyrolysis products.

Table 3 Limit of detection (LOD) for eight common polymer and associate theoretical estimate size of identifiable particle, in the form of sphere, fiber and fragment.

		Theoretical size		
Polymer	**LOD (in µg)**	**Sphere diameter (in µm)** [d]	**Fiber length (in µm)** [d e]	**Fragment length (in µm)** [d f]
PE[a]	0.070	51.7	229.9	28.9
PS[a]	0.003	17.7	9.2	1.2
PMMA[a]	0.029	35.9	77.2	9.7
PA-6[b]	0.110	57.1	309.9	38.9
PP[b]	0.027	38.6	95.5	12.0
PET[b]	0.015	27.4	34.1	4.3
PC[c]	0.116	35.9	77.0	9.7
uPVC[c]	0.592	58.7	366.6	42.3

[a] Polymer used in form of microspheres ;[b] Polymer used in form of filaments; [c] Polymer used in form of fragments; [d] LOD in size for sphere. fiber and fragment were calculated based on LOD in weight; [e] Calculation made with a diameter of 20 µm; [f] Calculation made based on a parallelepipoid form with 50 µm as side size.

To date, identification of isolated MP using Py-GC/MS was successful for particles with a size down to 100 µm [19] and down to 0.4 µg [22]. Here, uPVC demonstrated the highest LOD with 0.592 µg. This could be explained by uPVC fragment form and important density. Indeed, uPVC particles were thick (≈ 310 µm) and long (195 to 220 µm) leading to heavy particles (> 20 µg) due to its important density (1.4 g cm^{-3}) leading to an heavy estimated weight in comparison with other polymers. Globally, polymers with the highest densities, PA-6, PC or uPVC, have the highest LOD (Table 3). In the present study, estimated weight of the particles used for optimization and performance assessment were below 10 µg with the exception of uPVC particles and were even below 1 µg for some polymers (*i.e.* PS and PP). Furthermore, in previous works, Py-GC/MS was successfully applied to identify particles weighting 20 µg [24] and below 10 µg [22]. Limit of detection expressed in µg were low and

403 demonstrate that this method is applicable to very small and light particles. In addition to
404 LOD in µm, theoretical identifiable size (in µm) were calculated for MP in form of spheres,
405 fibers and fragments for all 8 polymer tested in the present study (Table 3). Those theoretical
406 minimal identifiable sizes were calculated using the LOD expressed in mass, polymer density
407 and equation (1-3) (see Electronic Supplementary Material Weight Estimation). For spheres,
408 all identifiable size were below 60 µm in diameter, for fibers of 20 µm of diameter length size
409 varied from 9.2 µm to 366.6 µm and for fragment all length size were below 50 µm (Table 3).
410 Here, these theoretical sizes showed that fiber are the MP form with the longest size
411 identifiable with the optimized Py-GC/MS. Indeed, fibers are long but thin resulting in an
412 important considered size (as the longest size was selected) with a low estimated weight.
413 Moreover, as Py-GC/MS rely on particles weight, it is an important parameter to master in
414 MP research.

415 MP are commonly defined as plastic particles smaller than 5 mm [7]. However, recently,
416 some studies argue that plastic particles should be described using another parameter [42, 43].
417 Here, as stated by Simon et al, [43], weight was chosen as an additional parameter to record
418 during MP studies. Indeed, plastic including MP are three dimensions particles, the
419 description of such particles accordingly to their longest size is problematic and could not be
420 adequate for data interpretations [43]. Actually, it is easy to visualize that there is an
421 important difference in weight for a fiber measuring 500 µm in its longest size with few
422 microns of diameters and a cubic fragment measuring 500 µm for all its side. This difference
423 in weight could also have different adverse effect when these particles are, for example,
424 ingested by organisms. In addition, plastic emissions to the Oceans are estimate in weight [3]
425 and determining MP weight could help for further estimation of MP source and quantities in
426 the Oceans. In the present study, limit of detection of the optimized Py-GC/MS were
427 estimated in µg because this technique is dependent on the particle weight and not their size.

Moreover, in other studies using thermal analyses, MP could be directly quantified in samples as previously demonstrated [22, 44]. Nevertheless, in the present study such quantification was not the purpose of the work. For further studies, MP weight should be estimated using weighting if possible or using volume calculation followed by weight estimation using a range of polymer density or using density found in the literature, as done by Simon et al, [43].

However, before being submitted to Py-GC/MS analysis, particles have to be handled with tweezers and placed in an analysis cup. The main limitation with the presented method is the "handibility" of the particles. Below 50 µm it is very difficult to manipulate the particles as some particles may easily "fly away". Here, the device is not the limiting element whereas the operator is as almost all theoretical identifiable sizes are below 50 µm. Moreover, for application on unknown particles, the highest LOD have to be considered to ensure accurate identification. Consequently and to date, the effective lowest size for plastic identification with this Py-GC/MS method, using particle handling, was evaluated at 50 µm.

Nevertheless, Py-GC/MS has been used to identify nanometric size scale plastic from bulk sample [31]. This approach was made possible as it did not use direct particles handling due to their sizes and because a data statistical treatment was applied after acquisition of pyrograms [31]. If direct handling of particles is not use, Py-GC/MS could be applied to identify smaller plastic particles. Indeed, the use of flow-cytometry using sorting [45] could be used to place potential MP in analysis cup. Flow cytometry in combination with a camera and a cell sorter have been used to detect MP [46]. Another technique could be the use of staining techniques like Nile red [47-49] before Py-GC/MS analysis. Indeed, stained particles could be introduced in analysis cup directly with the filter, for example. Moreover, the use of fixing solution to trap MP could also be a solution to isolate this particle and placing them in the analysis cup. However, potential interference of these solutions be carefully controlled

before to be employed in routine. With Py-GC/MS, development to isolate particles should be performed to enhance particle handling and to ensure that the device is the only limitation.

3.3. Method comparison

Here particles were collected by hand on a local beach. Particles used to compare identifications between µ-Raman and Py-GC/MS were diverse in shapes and colors. The most common shape was fragments (21), followed by pellets (14), filaments (6), beads (5) and foams (4). Concerning particles color, green was the most common (8), followed by orange (7), blue (7), transparent (6), red (5), yellow (4), white (3), black (3), grey (3), purple (3), and pink (1).

Only forty out of fifty particles were identified with µ-Raman as plastic particles. From the ten particles not identified, four were identified as pigments containing particles (Cobalt and copper phthalocyanine and Mortoperm blue). Among the 40 identified particles, there was: PE (22), PP (11), PS (3), PE-PP copolymer (3), and polyamide (1) (Fig 3).

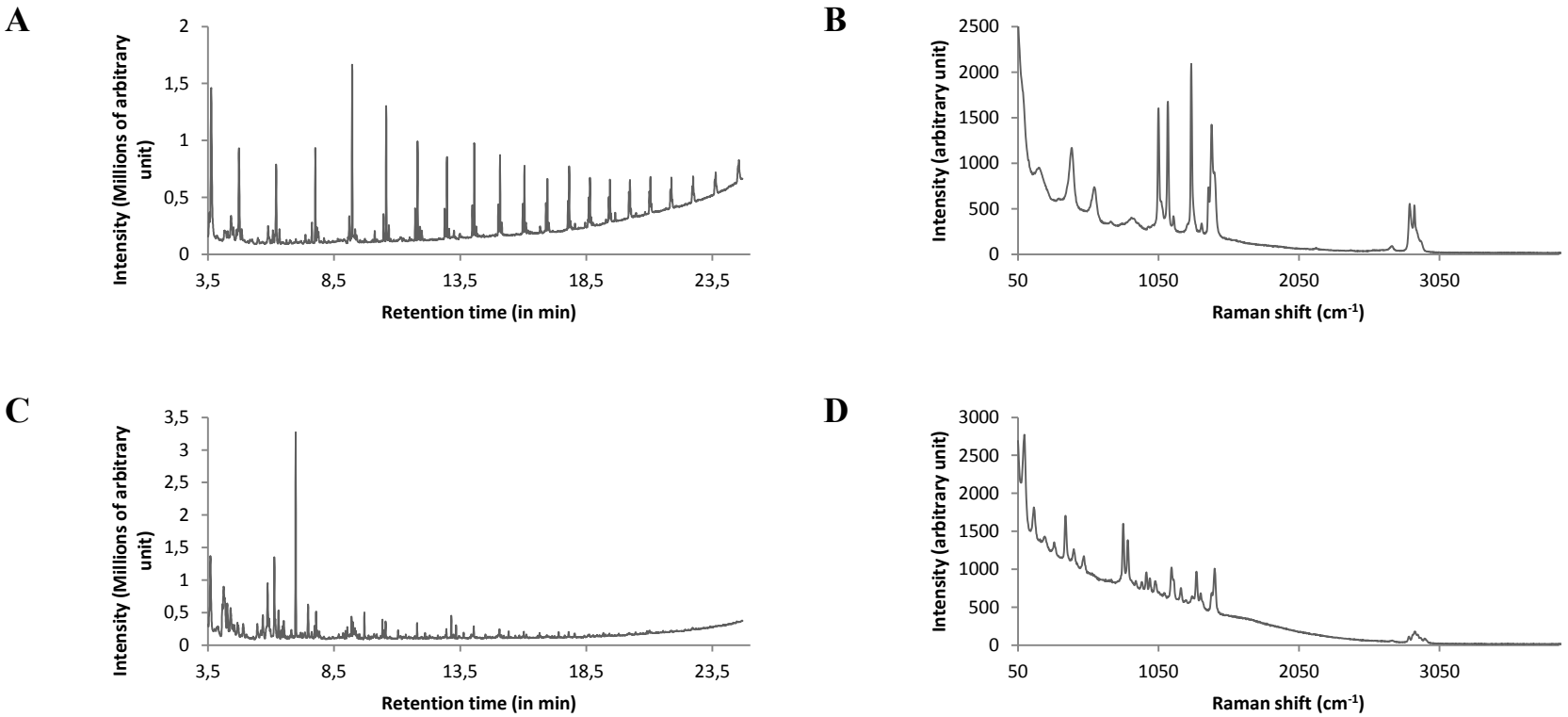

465 **Fig. 3 Pyrograms and Raman spectra acquired at 785 nm obtained from particles collected on a beach used for method comparison. Pyrogram and Raman spectra**
466 **respectively for a Polyethylene MP (A & B) and a Polypropylene MP (C & D).**

467

468 The optimized Py-GC/MS method also identified all the 40 particles. Thirty seven particles
469 (92 %) were identified as they were after µ-Raman analysis. Py-GC/MS led to results with a
470 finer identification, two PP particles being identified as PE-PP copolymer. Moreover, the
471 particle identified as polyamide with µ-Raman was identified as a copolymer made of PE, PP
472 and PA-6 (see Electronic Supplementary Material Figure S13). The optimized Py-GC/MS
473 method identified 100 % of the 40 previously identified particles with µ-Raman as plastic and
474 demonstrated that this method is reliable for MP identification.
475 Some particles were not identified with µ-Raman spectroscopy or were identified as
476 pigments. Pigment containing particles identification were also obtained in previous studies
477 on MP from water samples or marine organisms [16, 26-28]. Misidentification could occur for
478 these pigmented particles pigments due to an overlaying of the polymer signal by the additive
479 [11, 50]. Although some pigments are synthetic molecules, it could indicate a synthetic origin
480 but those particles could not be classified as plastic with certainty leading to potential
481 underestimation in field studies. Indeed some particle containing pigments could simply be
482 colorful paint particles as demonstrated by Imhof et al, [50]. Out of the 6 not identified
483 particles, 3 were discolored pellets. Discoloration indicates that pellets had a higher residence
484 time in the environment [51]. Additionally, Py-GC/MS could also be complementary to FTIR
485 to identified MP in field studies, as recently demonstrated [52]. Indeed, using FTIR polymer
486 signal could be overlap by some plastic additives included and identification could be
487 disturbed [53, 54]. In a recent study, Elert et al. [55] demonstrated that depending on the
488 require information on MP information, *i.e.* quantification or identification of polymers, the
489 appropriate technique should be used but the authors also indicated that identifications should
490 be used in complementarity. Raman, FTIR and Py-GC/MS are, to date, the major
491 identification techniques used in MP studies and those techniques are all complementary.

Then, the unidentified particles with μ-Raman spectroscopy were analyzed by Py-GC/MS and included in the application section (*cf.* 3.4).

3.4. Application: identification of unknown particles

On the sixty analyzed particles by Py-GC/MS, twenty (16 particles from bivalves and 4 from beach samples) formely identified as pigment containing particles by μ-Raman were processed by Py-GC/MS. All twenty particles were fragments with blue the dominant color with only one being green. Py-GC/MS identified 14 pigment particles as plastic polymers (70 %), 4 pigment particles as plastic polymers with some uncertainty (20 %) and 2 particles were not identified (10% - Fig. 4). PS was the most common identified polymer (13 particles out of 14) with one particle identified as a copolymer of PS and PMMA. Moreover, particles identified with uncertainty displayed characteristic compounds of PS but with low intensity. Here, Py-GC/MS identified 70 % of particles that were previously identified as pigment containing particles using μ-Raman. Moreover, μ-Raman only identified presence of the pigments nature as it overlaps with polymer signals, while Pyrolysis only allow to identify the native plastic polymer. Despite an effective lowest size of 50 μm, due to handling issue, being 10 to 50 times higher than the lowest size respectively analyzable by FTIR or μ-Raman spectroscopy, respectively, the Py-GC/MS method is still competitive and complementary. Indeed, as it allows (i) the full identification of pigments and some fibers and (ii) could be combined with improved separation methods to retrieve smaller particles. Here, Py-GC/MS could be used as a complementary identification method after μ-Raman spectroscopy.

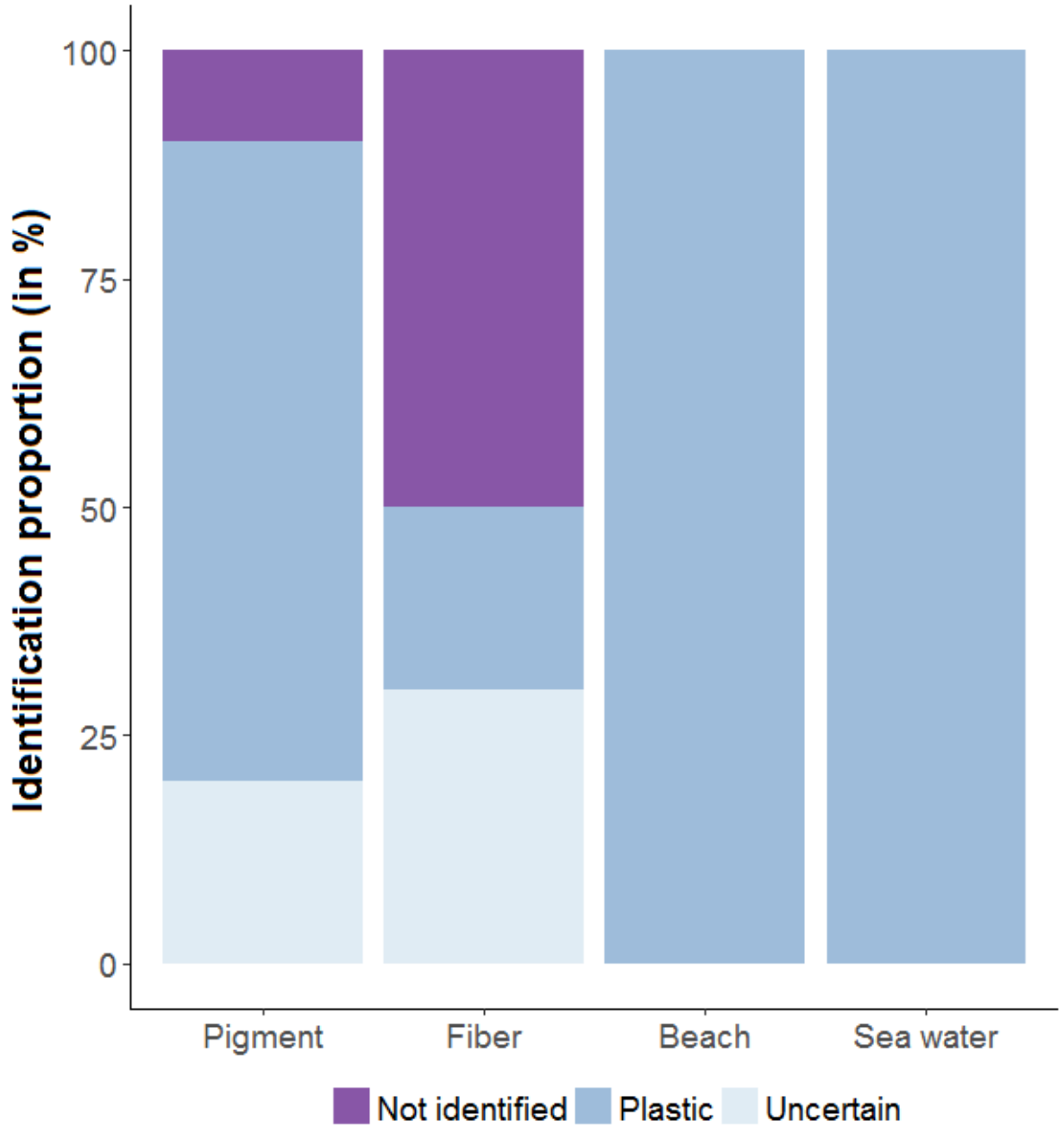

Fig. 4 Sample proportion for each identification class obtained after Py-GC/MS for particles previously identified as pigment (n=20) by µ Raman, fibers (n=10) and particles collected on a beach (n=6) and in surface sea water of the Bay of Brest (n=24). Not identified correspond to particles with low or no discernible signal, Uncertain to identification as plastic with some uncertainty and Plastic to identification with accurate polymer attribution

Out of the 10 fibers extracted from bivalves, 7 were blue, 2 were black, and 1 was red. For fibers, identification was achieved having 2 fibers identified as PE and Polyacrylonitrile (PAN). Fibers made of PAN, PE and potentially PET were identify and such polymer are commonly used in the textile industry [56] and are found in wastewater treatment plants after washing machine [57]. Three fibers were identified as plastic polymer with some uncertainty

and 5 fibers were not identified due to low or absent signal (Fig. 5). Uncertain identification for fibers comprised 1 PE and 2 PET. Fibers identification was tough. Indeed, only 20 % of the analyzed fibers were correctly identified. As fibers are long and thin, they are lighter in comparison with fragment. As Py-GC/MS rely more on particle weight than on their size, low weight could result in uncertainity with identifications, as previously observed for fibers in a study conducted by Hendrickson et al, [24]. To improve fibers and small particles identification, a solution could be the use of single ion monitoring (SIM) which target selected ion (m/z) allowing to decrease the LOD.

Out of the 30 others particles collected at sea-surface or in beach sediment, fragments (10) were the most common particles followed by foams (6), filaments (5), pellets (4), films (4), and beads (1). Regarding particles color: white was the dominant color (8) followed by blue (6), orange (5), transparent (5), green (3), red (1), black (1), and yellow (1). Particles were all identified as plastic with no uncertainty (Fig. 5) however it is important to indicate that the particule used in this section were large MP cut (*ca*. 200 µm) to be introduced in an analysis cup. PE (14) was the most common polymer followed by PP (9) and PS (4). Other polymers including PE-PP copolymer, Chlorinated PE (CPE), and Acrylonitrile-butadiene-styrene copolymer (ABS) were each found only once. Py-GC/MS provide good identification with similarity percentage above 80 %. The differentiation between PS and ABS remained difficult as both polymers are made with styrene which is the major characteristic compounds of their pyrograms [32, 33]. ABS reference presented an interesting characteristic compound: 1-Naphthalenecarbonitrile. This compound was only present in ABS reference pyrogram. Differentiation was made using this compound and tracking it in the pyrogram using its major ion: 153 m/z. Polymers identified *i.e.* PE, PP and PS are commonly reported on the beach [58] and in sea-surface water [38].

4. Conclusion

The present work described an in-depth optimization of a Py-GC/MS method to identify MP followed by an efficiency assessment of its performance and a comparison with Raman spectroscopic approach. In addition, to evaluate the robustness of the optimized Py-GC/MS method to identify MP, it was applied on samples from different matrices: bivalve, beach and sea-water surface. Optimization demonstrated that increasing pyrolysis temperature up to 700 °C in combination with a split ratio of 5 and an injector temperature set at 300 °C improved signal detection. Then, performance assessment demonstrated that if signal vary over time, such variation had no impact on MP identification. This method is validated on qualitative data but not on quantitative one due to RSD value above 20 % for repeatability and intermediate precision.

The optimized Py-GC/MS has some advantages in comparison with other MP identification methods. Firstly, Py-GC/MS is a complementary method to spectroscopy approaches. Indeed, in the present study Py-GC/MS enable identification of pigment containing particles right after µ-Raman analysis. Moreover Py-GC/MS identified co-polymer like PE-PP or PE-PP-PA6 which could be difficult to identify with µ-Raman without chemometrics approach. Secondly, up to date, Py-GC/MS identification of plastic particles cannot be done below 50 µm (longest size) not because of LOD but due to operator handling issues. A better way, like the introduction of a piece of filter on which particles are into the analysis cup, should be developed in order to avoid this limiting step. However, Py-GC/MS could be used to identify smaller particles, like nanoplastics as already demonstrated. By resolving this handling issue, LOD calculation demonstrated that this method could identify isolated MP weighting below 1 µg. In addition, another strategy that can be considered to lower the LOD for this Py-GC/MS method is the use of SIM. To get identification on MP polluting from both freshwater and marine environment, the use of Py-GC/MS should be better considered as this method prove

572 to be efficient in identifying MP from various matrices. In an effort to standardize the MP
573 analysis workflow, this method could be implemented either on its own or after FTIR or
574 Raman to confirm some identification or to circumvent unsuccessful spectroscopy
575 identification. Finally, MP mass should be evaluated in MP studies to try to standardized
576 leading to better comparison of MP contamination between studies.

577

Acknowledgments

Ludovic Hermabessiere is grateful to the Hauts-de-France Region and ANSES (French Agency for Food, Environmental and Occupational Health & Safety) for the financial support of his PhD. Maria Kazour is financially supported by a PhD fellowship from the National Council for Scientific Research (Lebanon) and Université du Littoral Côte d'Opale (France). This paper has been funded by the French National Research Agency (ANR) (ANR-15-CE34-0006-02), as part of the Nanoplastics project and also by the French government and the Hauts-de-France Region in the framework of the project CPER 2014-2020 MARCO.

This is a post-peer-review, pre-copyedit version of an article published in Analytical and Bioanalytical Chemistry. The final authenticated version is available online at: https://doi.org/10.1007/s00216-018-1279-0

Compliance with Ethical Standards

Conflict of Interest: Authors declare no conflict of interest.

References

1. Thompson, R.C., S.H. Swan, C.J. Moore, and F.S. vom Saal, 2009. Our plastic age. Philosophical Transactions of the Royal Society B: Biological Sciences. 364, 1973-1976. doi: 10.1098/rstb.2009.0054
2. PlasticsEurope, 2018. Plastics – the Facts 2017: An analysis of European plastics production, demand and waste data. Available on: http://www.plasticseurope.fr/Document/plastics---the-facts-2017.aspx?FolID=2, Accessed on: 01/29/2018
3. Jambeck, J.R., R. Geyer, C. Wilcox, T.R. Siegler, M. Perryman, A. Andrady, R. Narayan, and K.L. Law, 2015. Plastic waste inputs from land into the ocean. Science. 347, 768-771. doi: 10.1126/science.1260352
4. Cózar, A., F. Echevarría, J.I. González-Gordillo, X. Irigoien, B. Úbeda, S. Hernández-León, Á.T. Palma, S. Navarro, J. García-de-Lomas, A. Ruiz, M.L. Fernández-de-Puelles, and C.M. Duarte, 2014. Plastic debris in the open ocean. Proceedings of the National Academy of Sciences. 111, 10239-10244. doi: 10.1073/pnas.1314705111
5. Eriksen, M., L.C. Lebreton, H.S. Carson, M. Thiel, C.J. Moore, J.C. Borerro, F. Galgani, P.G. Ryan, and J. Reisser, 2014. Plastic pollution in the world's oceans: more

than 5 trillion plastic pieces weighing over 250,000 tons afloat at sea. PloS one. 9, e111913.
6. van Sebille, E., C. Wilcox, L. Lebreton, N. Maximenko, B.D. Hardesty, J.A. van Franeker, M. Eriksen, D. Siegel, F. Galgani, and K.L. Law, 2015. A global inventory of small floating plastic debris. Environmental Research Letters. 10, 124006.
7. Arthur, C., J. Baker, and H. Bamford, 2009. International Research Workshop on the Occurrence, Effects, and Fate of Microplastic Marine Debris. NOAA Technical Memorandum NOS-OR&R-30.
8. Li, W.C., H.F. Tse, and L. Fok, 2016. Plastic waste in the marine environment: A review of sources, occurrence and effects. Science of The Total Environment. 566–567, 333-349. doi: 10.1016/j.scitotenv.2016.05.084
9. Horton, A.A., A. Walton, D.J. Spurgeon, E. Lahive, and C. Svendsen, 2017. Microplastics in freshwater and terrestrial environments: Evaluating the current understanding to identify the knowledge gaps and future research priorities. Science of The Total Environment. 586, 127-141. doi: 10.1016/j.scitotenv.2017.01.190
10. Imhof, H.K., J. Schmid, R. Niessner, N.P. Ivleva, and C. Laforsch, 2012. A novel, highly efficient method for the separation and quantification of plastic particles in sediments of aquatic environments. Limnology and Oceanography: Methods. 10, 524-537. doi: 10.4319/lom.2012.10.524
11. Lenz, R., K. Enders, C.A. Stedmon, D.M.A. Mackenzie, and T.G. Nielsen, 2015. A critical assessment of visual identification of marine microplastic using Raman spectroscopy for analysis improvement. Marine Pollution Bulletin. 100, 82-91. doi: 10.1016/j.marpolbul.2015.09.026
12. Shim, W.J., S.H. Hong, and S.E. Eo, 2017. Identification methods in microplastic analysis: a review. Analytical Methods. 9, 1384-1391. doi: 10.1039/C6AY02558G
13. CAMPUS, 2018. Available on: https://www.campusplastics.com/campus/list, Accessed on: 01/26/2018
14. Remy, F., F. Collard, B. Gilbert, P. Compère, G. Eppe, and G. Lepoint, 2015. When Microplastic Is Not Plastic: The Ingestion of Artificial Cellulose Fibers by Macrofauna Living in Seagrass Macrophytodetritus. Environmental Science & Technology. 49, 11158-11166. doi: 10.1021/acs.est.5b02005
15. Rocha-Santos, T. and A.C. Duarte, 2015. A critical overview of the analytical approaches to the occurrence, the fate and the behavior of microplastics in the environment. Trends in Analytical Chemistry. 65, 47-53. doi: 10.1016/j.trac.2014.10.011
16. Frère, L., I. Paul-Pont, J. Moreau, P. Soudant, C. Lambert, A. Huvet, and E. Rinnert, 2016. A semi-automated Raman micro-spectroscopy method for morphological and chemical characterizations of microplastic litter. Marine Pollution Bulletin. 113, 461-468. doi: 10.1016/j.marpolbul.2016.10.051
17. Oßmann, B.E., G. Sarau, S.W. Schmitt, H. Holtmannspötter, S.H. Christiansen, and W. Dicke, 2017. Development of an optimal filter substrate for the identification of small microplastic particles in food by micro-Raman spectroscopy. Analytical and Bioanalytical Chemistry. 409, 4099-4109. doi: 10.1007/s00216-017-0358-y
18. Phuong, N.N., A. Zalouk-Vergnoux, A. Kamari, C. Mouneyrac, F. Amiard, L. Poirier, and F. Lagarde, 2017. Quantification and characterization of microplastics in blue mussels (*Mytilus edulis*): protocol setup and preliminary data on the contamination of the French Atlantic coast. Environmental Science and Pollution Research, 1-10. doi: 10.1007/s11356-017-8862-3

19. Dekiff, J.H., D. Remy, J. Klasmeier, and E. Fries, 2014. Occurrence and spatial distribution of microplastics in sediments from Norderney. Environmental Pollution. 186, 248-256. doi: 10.1016/j.envpol.2013.11.019
20. Fries, E., J.H. Dekiff, J. Willmeyer, M.-T. Nuelle, M. Ebert, and D. Remy, 2013. Identification of polymer types and additives in marine microplastic particles using pyrolysis-GC/MS and scanning electron microscopy. Environmental Science: Processes & Impacts. 15, 1949-1956. doi: 10.1039/C3EM00214D
21. Nuelle, M.-T., J.H. Dekiff, D. Remy, and E. Fries, 2014. A new analytical approach for monitoring microplastics in marine sediments. Environmental Pollution. 184, 161-169. doi: 10.1016/j.envpol.2013.07.027
22. Fischer, M. and B.M. Scholz-Böttcher, 2017. Simultaneous Trace Identification and Quantification of Common Types of Microplastics in Environmental Samples by Pyrolysis-Gas Chromatography–Mass Spectrometry. Environmental Science & Technology. 51, 5052-5060. doi: 10.1021/acs.est.6b06362
23. Fabbri, D., D. Tartari, and C. Trombini, 2000. Analysis of poly(vinyl chloride) and other polymers in sediments and suspended matter of a coastal lagoon by pyrolysis-gas chromatography-mass spectrometry. Analytica Chimica Acta. 413, 3-11. doi: 10.1016/S0003-2670(00)00766-2
24. Hendrickson, E., E.C. Minor, and K. Schreiner, 2018. Microplastic abundance and composition in western Lake Superior as determined via microscopy, Pyr-GC/MS, and FTIR. Environmental Science & Technology. 52, 1787-1796. doi: 10.1021/acs.est.7b05829
25. Ceccarini, A., A. Corti, F. Erba, F. Modugno, J. La Nasa, S. Bianchi, and V. Castelvetro, 2018. The hidden microplastics. New insights and figures from the thorough separation and characterization of microplastics and of their degradation by-products in coastal sediments. Environmental Science & Technology. doi: 10.1021/acs.est.8b01487
26. Van Cauwenberghe, L., M. Claessens, M.B. Vandegehuchte, and C.R. Janssen, 2015. Microplastics are taken up by mussels (*Mytilus edulis*) and lugworms (*Arenicola marina*) living in natural habitats. Environmental Pollution. 199, 10-17. doi: 10.1016/j.envpol.2015.01.008
27. Van Cauwenberghe, L. and C.R. Janssen, 2014. Microplastics in bivalves cultured for human consumption. Environmental Pollution. 193, 65-70. doi: 10.1016/j.envpol.2014.06.010
28. Schymanski, D., C. Goldbeck, H.-U. Humpf, and P. Fürst, 2018. Analysis of microplastics in water by micro-Raman spectroscopy: Release of plastic particles from different packaging into mineral water. Water Research. 129, 154-162. doi: 10.1016/j.watres.2017.11.011
29. Li, J., H. Liu, and J. Paul Chen, 2018. Microplastics in freshwater systems: A review on occurrence, environmental effects, and methods for microplastics detection. Water Research. 137, 362-374. doi: 10.1016/j.watres.2017.12.056
30. Ivleva, N.P., A.C. Wiesheu, and R. Niessner, 2016. Microplastic in Aquatic Ecosystems. Angewandte Chemie International Edition. 56, 1720-1739. doi: 10.1002/anie.201606957
31. Ter Halle, A., L. Jeanneau, M. Martignac, E. Jardé, B. Pedrono, L. Brach, and J. Gigault, 2017. Nanoplastic in the North Atlantic Subtropical Gyre. Environmental Science & Technology. 51, 13689-13697. doi: 10.1021/acs.est.7b03667
32. Tsuge, S., H. Ohtani, and C. Watanabe, *Pyrolysis-GC/MS Data Book of Synthetic Polymers*. 2011: Elsevier. 390.

33. Kusch, P., *Application of Pyrolysis-Gas Chromatography/Mass Spectrometry (Py-GC/MS)*, in *Characterization and Analysis of Microplastics*, T. Rocha-Santos and A. Duarte, Editors. 2016, Elsevier. p. 306.
34. van Den Dool, H. and P.D. Kratz, 1963. A generalization of the retention index system including linear temperature programmed gas—liquid partition chromatography. Journal of Chromatography A. 11, 463-471. doi: 10.1016/S0021-9673(01)80947-X
35. Dehaut, A., A.-L. Cassone, L. Frère, L. Hermabessiere, C. Himber, E. Rinnert, G. Rivière, C. Lambert, P. Soudant, A. Huvet, G. Duflos, and I. Paul-Pont, 2016. Microplastics in seafood: Benchmark protocol for their extraction and characterization. Environmental Pollution. 215, 223-233. doi: 10.1016/j.envpol.2016.05.018
36. International Organization for Standardization (ISO), 1994. 5725-3: 1994, Accuracy (trueness and precision) of measurement methods and results-Part 3: Intermediate measures of the precision of a standard measurement method. International Organization for Standardization, Geneva.
37. Caporal-Gautier, J., M. Nivet J, P. Algranti, M. Guilloteau, M. Histe, M. Lallier, J. N'Guyen-Huu J, and R. Russotto, 1992. Guide de validation analytique. Rapport d'une commission SFSTP. I : Méthodologie. STP pharma pratiques. 2, 205-226.
38. Frère, L., I. Paul-Pont, E. Rinnert, S. Petton, J. Jaffré, I. Bihannic, P. Soudant, C. Lambert, and A. Huvet, 2017. Influence of environmental and anthropogenic factors on the composition, concentration and spatial distribution of microplastics: A case study of the Bay of Brest (Brittany, France). Environmental Pollution. 225, 211-222. doi: https://doi.org/10.1016/j.envpol.2017.03.023
39. R Core Team, 2015. R: A language and environment for statistical computing. Vienna, Austria; 2014. Available on: http://www.R-project.org, Accessed on: 10/15/2015
40. De Mendiburu, F., 2014. Agricolae: statistical procedures for agricultural research. R package version.
41. McGuffin, V.L., *Theory of chromatography*, in *Journal of Chromatography Library*. 2004, Elsevier. p. 1-93.
42. Filella, M., 2015. Questions of size and numbers in environmental research on microplastics: methodological and conceptual aspects. Environmental Chemistry. 12, 527-538. doi: 10.1071/EN15012
43. Simon, M., N. van Alst, and J. Vollertsen, 2018. Quantification of microplastic mass and removal rates at wastewater treatment plants applying Focal Plane Array (FPA)-based Fourier Transform Infrared (FT-IR) imaging. Water Research. 142, 1-9. doi: 10.1016/j.watres.2018.05.019
44. Dümichen, E., A.-K. Barthel, U. Braun, C.G. Bannick, K. Brand, M. Jekel, and R. Senz, 2015. Analysis of polyethylene microplastics in environmental samples, using a thermal decomposition method. Water Research. 85, 451-457. doi: 10.1016/j.watres.2015.09.002
45. Ibrahim, S.F. and G. van den Engh, *Flow Cytometry and Cell Sorting*, in *Cell Separation: Fundamentals, Analytical and Preparative Methods*, A. Kumar, I.Y. Galaev, and B. Mattiasson, Editors. 2007, Springer Berlin Heidelberg: Berlin, Heidelberg. p. 19-39.
46. Sgier, L., R. Freimann, A. Zupanic, and A. Kroll, 2016. Flow cytometry combined with viSNE for the analysis of microbial biofilms and detection of microplastics. Nature communications. 7, 11587.
47. Shim, W.J., Y.K. Song, S.H. Hong, and M. Jang, 2016. Identification and quantification of microplastics using Nile Red staining. Marine Pollution Bulletin. 113, 469-476. doi: 10.1016/j.marpolbul.2016.10.049

48. Maes, T., R. Jessop, N. Wellner, K. Haupt, and A.G. Mayes, 2017. A rapid-screening approach to detect and quantify microplastics based on fluorescent tagging with Nile Red. Scientific Reports. 7, 44501. doi: 10.1038/srep44501
49. Erni-Cassola, G., M.I. Gibson, R.C. Thompson, and J.A. Christie-Oleza, 2017. Lost, but Found with Nile Red: A Novel Method for Detecting and Quantifying Small Microplastics (1 mm to 20 μm) in Environmental Samples. Environmental Science & Technology. 51, 13641-13648. doi: 10.1021/acs.est.7b04512
50. Imhof, H.K., C. Laforsch, A.C. Wiesheu, J. Schmid, P.M. Anger, R. Niessner, and N.P. Ivleva, 2016. Pigments and plastic in limnetic ecosystems: A qualitative and quantitative study on microparticles of different size classes. Water Research. 98, 64-74. doi: 10.1016/j.watres.2016.03.015
51. Endo, S., R. Takizawa, K. Okuda, H. Takada, K. Chiba, H. Kanehiro, H. Ogi, R. Yamashita, and T. Date, 2005. Concentration of polychlorinated biphenyls (PCBs) in beached resin pellets: Variability among individual particles and regional differences. Marine Pollution Bulletin. 50, 1103-1114. doi: 10.1016/j.marpolbul.2005.04.030
52. Käppler, A., M. Fischer, B.M. Scholz-Böttcher, S. Oberbeckmann, M. Labrenz, D. Fischer, K.-J. Eichhorn, and B. Voit, 2018. Comparison of μ-ATR-FTIR spectroscopy and py-GCMS as identification tools for microplastic particles and fibers isolated from river sediments. Analytical and Bioanalytical Chemistry. doi: 10.1007/s00216-018-1185-5
53. Tabb, D.L. and J.L. Koenig, 1975. Fourier Transform Infrared Study of Plasticized and Unplasticized Poly(vinyl chloride). Macromolecules. 8, 929-934. doi: 10.1021/ma60048a043
54. González, N. and M.J. Fernández-Berridi, 2006. Application of Fourier transform infrared spectroscopy in the study of interactions between PVC and plasticizers: PVC/plasticizer compatibility versus chemical structure of plasticizer. Journal of Applied Polymer Science. 101, 1731-1737. doi: doi:10.1002/app.23381
55. Elert, A.M., R. Becker, E. Duemichen, P. Eisentraut, J. Falkenhagen, H. Sturm, and U. Braun, 2017. Comparison of different methods for MP detection: What can we learn from them, and why asking the right question before measurements matters? Environmental Pollution. 231, 1256-1264. doi: 10.1016/j.envpol.2017.08.074
56. Napper, I.E. and R.C. Thompson, 2016. Release of synthetic microplastic plastic fibres from domestic washing machines: Effects of fabric type and washing conditions. Marine Pollution Bulletin. 112, 39-45. doi: https://doi.org/10.1016/j.marpolbul.2016.09.025
57. Browne, M.A., P. Crump, S.J. Niven, E. Teuten, A. Tonkin, T. Galloway, and R. Thompson, 2011. Accumulation of Microplastic on Shorelines Woldwide: Sources and Sinks. Environmental Science & Technology. 45, 9175-9179. doi: 10.1021/es201811s
58. Lots, F.A.E., P. Behrens, M.G. Vijver, A.A. Horton, and T. Bosker, 2017. A large-scale investigation of microplastic contamination: Abundance and characteristics of microplastics in European beach sediment. Marine Pollution Bulletin. 123, 219-226. doi: https://doi.org/10.1016/j.marpolbul.2017.08.057